Unclassified

SECURITY CLASSIFICATION OF THIS PAGE

(1)

REPORT DOCUMENTATION PAGE

AD-A211 873

1a. REPORT SECURITY CLASSIFICATION Unclassified	1b. RESTRICTIVE MARKINGS
2a. SECURITY CLASSIFICATION AUTHORITY	3. DISTRIBUTION / AVAILABILITY OF REPORT Approved for public release; Distribution unlimited
2b. DECLASSIFICATION / DOWNGRADING SCHEDULE	
4. PERFORMING ORGANIZATION REPORT NUMBER(S) GL-TR-89-0219	5. MONITORING ORGANIZATION REPORT NUMBER(S)
6a. NAME OF PERFORMING ORGANIZATION Geophysics Laboratory 6b. OFFICE SYMBOL (If applicable) PHP	7a. NAME OF MONITORING ORGANIZATION
6c. ADDRESS (City, State, and ZIP Code) Hanscom AFB Massachusetts 01731-5000	7b. ADDRESS (City, State, and ZIP Code)
8a. NAME OF FUNDING / SPONSORING ORGANIZATION 8b. OFFICE SYMBOL (If applicable)	9. PROCUREMENT INSTRUMENT IDENTIFICATION NUMBER
8c. ADDRESS (City, State, and ZIP Code)	10. SOURCE OF FUNDING NUMBERS PROGRAM ELEMENT NO. 62101F; PROJECT NO. 7601; TASK NO. 22; WORK UNIT ACCESSION NO. 01

DTIC FILE COPY

DTIC ELECTE AUG 28 1989 S D

11. TITLE (Include Security Classification)
Polar Rain and the Question of Direct Particle Access

12. PERSONAL AUTHOR(S)
M.S. Gussenhoven

13a. TYPE OF REPORT	13b. TIME COVERED	14. DATE OF REPORT (Year, Month, Day)	15. PAGE COUNT
Reprint	FROM _____ TO _____	1989 August 21	18

16. SUPPLEMENTARY NOTATION
Reprinted from Electromagnetic Coupling in the Polar Clefts and Caps, 43-60, P.E. Sandholt and A. Egeland (eds.) 1989

17. COSATI CODES		
FIELD	GROUP	SUB-GROUP

18. SUBJECT TERMS (Continue on reverse if necessary and identify by block number)
Polar rain; Electron precipitation; Magnetotail; Polar caps; Reprints (11.2)

19. ABSTRACT (Continue on reverse if necessary and identify by block number)

ABSTRACT: Recent experimental findings on the weak, low-energy electron population found in the tail lobes and the low altitude polar regions to which they magnetically map are reviewed in light of two different polar rain models. In one model the field aligned solar wind electrons have direct entry to the magnetosphere in the distant tail where the field lines are assumed to be open. In the other, the polar rain is the potential-barrier-reflected electron component of the magnetosheath population that enters the magnetosphere at the cusp, and perhaps all along the magnetopause. The data do not fully support one model over the other, and it is possible that both entry mechanisms contribute depending on magnetopause position, on electron energy, and on the size and extent of boundary and barrier potentials. Keywords:

20. DISTRIBUTION / AVAILABILITY OF ABSTRACT	21. ABSTRACT SECURITY CLASSIFICATION
☐ UNCLASSIFIED/UNLIMITED ☒ SAME AS RPT. ☐ DTIC USERS	Unclassified
22a. NAME OF RESPONSIBLE INDIVIDUAL M.S. Gussenhoven	22b. TELEPHONE (Include Area Code) (617) 377-3212 22c. OFFICE SYMBOL PHP

DD FORM 1473, 84 MAR 83 APR edition may be used until exhausted. All other editions are obsolete.

SECURITY CLASSIFICATION OF THIS PAGE
Unclassified

89 8 25 052

GL-TR-89-0219

POLAR RAIN AND THE QUESTION OF DIRECT PARTICLE ACCESS

M.S. Gussenhoven
Air Force Geophysics Laboratory
Hanscom AFB, MA 01731

ABSTRACT. Recent experimental findings on the weak, low-energy electron population found in the tail lobes and the low altitude polar regions to which they magnetically map are reviewed in light of two different polar rain models. In one model the field aligned solar wind electrons have direct entry to the magnetosphere in the distant tail where the field lines are assumed to be open. In the other, the polar rain is the potential-barrier-reflected electron component of the magnetosheath population that enters the magnetosphere at the cusp, and perhaps all along the magnetopause. The data do not fully support one model over the other, and it is possible that both entry mechanisms contribute depending on magnetopause position, on electron energy, and on the size and extent of boundary and barrier potentials.

1. INTRODUCTION

Winningham and Heikkila (1974) first identified and named polar rain in low altitude observations as a near-background, structureless, low-energy electron population that precipitates over the 'unperturbed' polar caps. Polar rain is of interest to the community of magnetospheric researchers because it is a distinct magnetospheric population with entry, transport and precipitation mechanisms that require explanation, because it carries information about its source or sources, and because it carries information about the distant tail magnetic field configuration and the interplanetary magnetic field. Two models have been proposed for the entry and transport of polar rain. In each the solar wind is the ultimate source.

In the 'direct entry' model, illustrated in Figure 1, the solar wind electron population is assumed to enter the magnetosphere along open field lines (field lines with one foot terminating in the Earth and the other in the solar wind). It is then adiabatically transported directly along these field lines to the low altitude polar caps. There is no significant heating of the solar wind plasma in the vicinity of the Earth as, say, in the magnetosheath. Electrons streaming away from the sun will enter the northern (southern) polar cap when the IMF is directed away from (toward) the sun while particles backstreaming

P. E. Sandholt and A. Egeland (eds.), Electromagnetic Coupling in the Polar Clefts and Caps, 43–60.
© 1989 by Kluwer Academic Publishers.

toward the sun will enter the southern (northern) polar cap. An analogy for this model is relativistic solar electron entry and transport (Paulikas, 1974). Fairfield and Scudder (1985) quantitatively extended the model to the solar wind and polar rain energy range.

The solar wind electron population that gains entry in this model has two components, an isotropic core with average temperature and density, 10±2 eV and 10±5 cm^{-3}, respectively, and a hotter halo population of 60±9 eV and .57±.23 cm^{-3} (Feldman et al., 1975). The pitch angle distribution of the halo population varies from isotropic to highly peaked along the field line in the direction away from the sun (Pilipp et al., 1987a,b). When the halo population is highly anisotropic it is referred to as the strahl because it is thought to proceed virtually unscattered from the sun to the near-Earth region (Olbert, 1981). A cut in the measured solar wind electron distribution function along the magnetic field, taken from Pilipp et al. (1987a), is shown in Figure 2 for the case of a highly anisotropic strahl. In the energy range 100-400 eV [$(6\text{-}12)10^5$ km/s] the ratio of fluxes in the direction away from to that toward the sun is more than two orders of magnitude. For direct entry this anisotropy will be carried unchanged into the magnetosphere. In Figure 1 the tear-drop shapes represent a highly anisotropic solar wind distribution function such that quite different fluxes are incident upon the two hemispheres. The portions of the distributions that are blocked by the magnetosphere have dashed lines. Since the magnetic field increases by several orders of magnitude from the magnetopause to the ionosphere, only particles in a loss cone of $\sim 1^\circ$ at the magnetopause will reach low altitudes before mirroring and returning to the distant tail or plasma sheet. Thus in the direct entry model, polar rain is only associated with the most field-aligned population in the solar wind (Fairfield and Scudder, 1985; Gosling et al., 1986, Baker et al., 1986).

The direct entry model predicts that for conditions of highly anisotropic strahl the polar rain flux in the hemisphere that receives electrons directed away from the sun (referred to throughout the remainder of the paper as the 'preferred hemisphere') should have stronger field alignment and greater intensity than in the opposite hemisphere (the 'non-preferred' hemisphere). For conditions of isotropic solar wind the fluxes in the two caps should be identical. Pilipp et al. (1987b) found that a narrowly peaked strahl occurs in the center of a sector coincident with the sector's high speed stream, that a broadly peaked strahl occurs at the trailing edge of the high speed stream and that the isotropic distribution occurs at a sector boundary.

The second model, called here the 'internal barrier' model and illustrated in Figure 3, was put forth by Foster and Burrows (1976, 1977) to explain infrequent, intense fluxes of keV electrons that have the same spatial smoothness as polar rain and no apparent counterpart in the solar wind. In their model the source of 'normal polar rain' is the magnetosheath. Magnetosheath electrons enter the magnetosphere with ions in the region of the cusp. Most of the inflowing cusp population mirrors and flows away from the Earth but remains within the

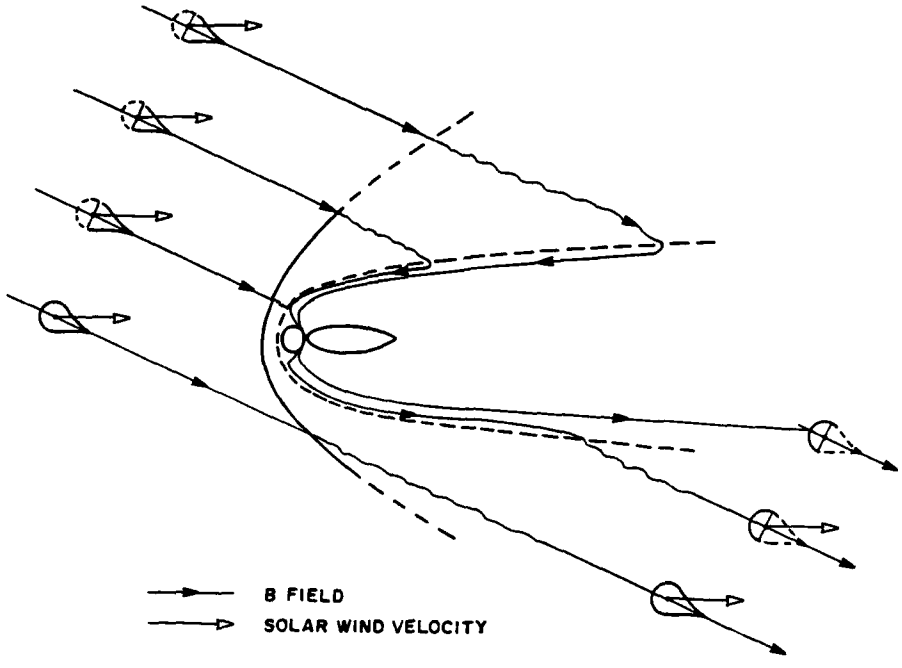

Figure 1. Schematic diagram of the direct entry model for polar rain.

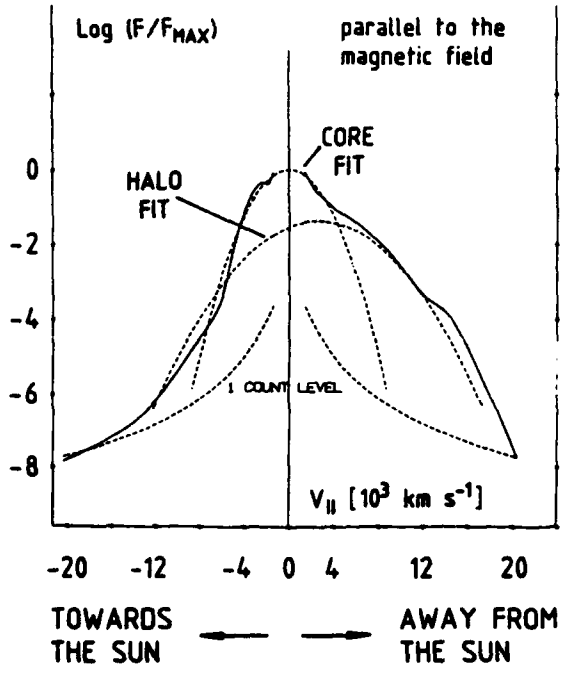

Figure 2. Highly anisotropic solar wind distribution function.

Codes
Dist | Avail and/or Special
A-1 | 20

magnetosphere due to the cross-cap convection electric field (Pilipp and Morfill, 1978). The outward flowing magnetosheath population is called the plasma mantle because it coats the tail lobe region just inside the magnetopause (Rosenbauer et al., 1975). This mantle population has been measured out to lunar distances. (See review by Sckopke and Paschmann, 1978). The extent to which it has expanded toward the plasma sheet at lunar distances is controlled by the IMF sector (Hardy et al., 1979a). Mantle plasma is preferentially seen at lunar distances in the morning (evening) sector in the northern (southern) hemisphere during away sectors and vice versa for toward sectors.

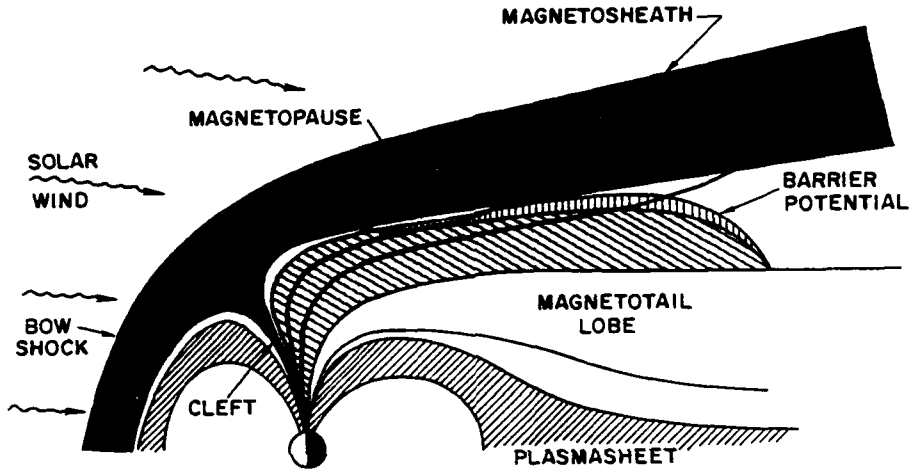

Figure 3. Schematic diagram of the internal barrier model of polar rain transport in the tail lobes.

In the Foster and Burrows picture an electrostatic barrier reflects a portion of the mantle electron population as polar rain. Occasionally the barrier is sufficiently large and widespread to accelerate distant tail lobe populations toward the cap to create intense, keV fluxes. The source for the electrostatic barrier is not identified. In the internal barrier model the polar rain distribution function is not directly comparable to the solar wind electron spectrum, but is a magnetosheath-like distribution modified by transport through a spatially-varying, field-aligned potential. Comparison of distribution functions in the near and distant tail lobes should reflect the existence of the total potential drop between the two positions.

In the following the characteristics of tail lobe electrons are reviewed in light of these two models. Measurements are organized by altitude starting with low altitudes, below several RE (RE = Earth radius), where the great majority of polar rain observations have been made; continuing through mid-range altitudes (5-60 RE); and ending with distant (>180 RE) tail lobe populations. The discussion will be

confined, unless otherwise stated, to electrons in the energy range between approximately 50 eV and 1 keV. This is also the typical energy range for solar wind halo (strahl) electrons. Altitude comparisons of densities and temperatures will be made for Maxwellian fits to electron spectra in this energy range.

2. POLAR RAIN CHARACTERISTICS AT LOW ALTITUDES

Polar rain is identified at low altitudes by its position above the auroral oval, and its large-scale spatial/temporal homogeneity. Three types of electron precipitation are typically found in the polar caps: polar rain, polar showers and polar cap arcs. These and their ion counterparts are illustrated in Figure 4. Here the electron number flux (left hand side) and ion number flux (right hand side) from 100-1000 eV are shown for three pre-noon to pre-midnight DMSP passes over the auroral regions and polar caps at 840 km on three days in April, 1985. The hourly averaged values of the three interplanetary magnetic field (IMF) components and KP are listed to the right. In the top electron panel the region of slowly varying electron precipitation in the polar cap (above ~75° MLAT) is polar rain. In the middle panel the electron precipitation in the highest latitude regions is designated polar showers and is characterized by high spatial (or temporal) variability. In the bottom panel the large blocks of intense electron precipitation extending to very high latitudes from the midnight region produce polar cap arcs. Polar rain most commonly occurs under conditions producing an active auroral oval, or when the IMF has a southward component; polar showers and polar cap arcs occur preferentially when the IMF has a northward component (Gussenhoven, 1982, Hardy, 1984).

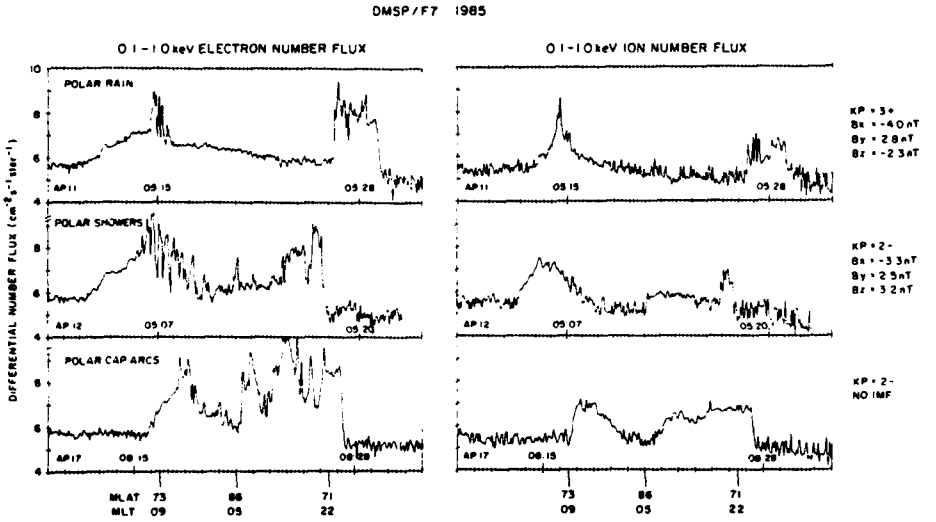

Figure 4. Precipitating electrons at low altitudes for three states of the polar cap.

The right hand panels in Figure 4 show the corresponding ion precipitation. In polar rain the ion precipitation is near background except behind the cleft (or dayside boundary layer). For conditions of polar showers and polar cap arcs significant ion precipitation is observed to very high latitudes, particularly on the nightside.

The low-altitude spectral characteristics of polar rain were quantified by Riehl and Hardy (1986) using 262 polar passes of DMSP data. Figure 5 shows the distribution function of a typical polar rain spectrum averaged over 45 seconds and fit to two Maxwellians in the energy ranges below and above approximately 1 keV. The great majority (70%) of the polar rain spectra examined by Riehl and Hardy did not have a high-energy component. For their data sample the distribution of polar rain temperatures fell mainly in the energy range 60-100 eV. The average value was found to be 80±13 eV which is 40% higher than the average solar wind halo population. The average density of the low energy polar rain component was found to be .055±.038 cm^{-3}, an order of magnitude smaller than the halo population. This comparison of average values strongly suggests that the entry and transport of solar wind electrons into and within the magnetosphere is not direct, but that heating and redistribution is part of the process. The pitch angle distributions of polar rain electrons at low altitude have not been studied systematically. Early observations suggest that it is isotropic over the down-coming hemisphere (Winningham and Heikkila, 1974).

Low altitude studies comparing the northern and southern polar rain flux levels on a daily basis show that there is almost always a higher flux in the preferred hemisphere for direct entry of fluxes streaming away from the sun: northern (southern) hemisphere for IMF away (toward) sectors (Fennell et al., 1975, Meng and Kroehl, 1977,

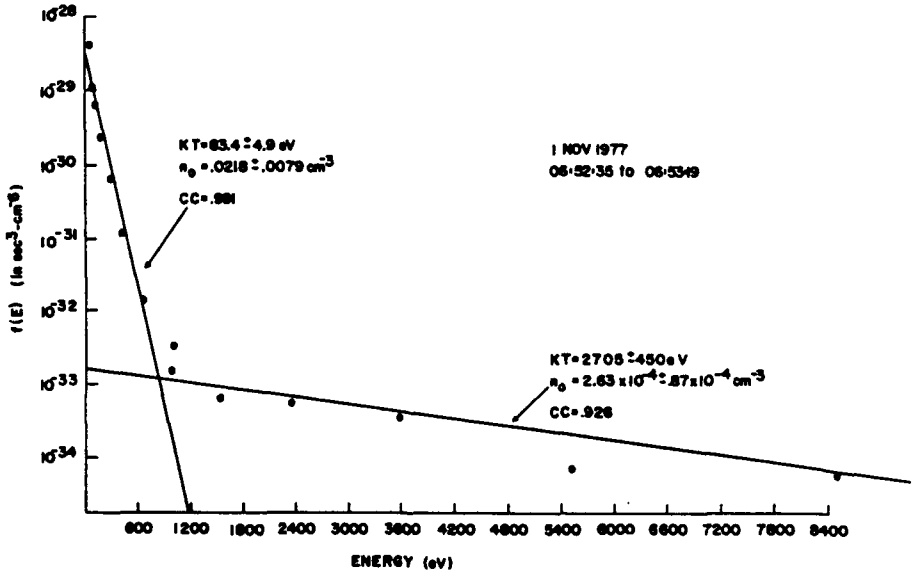

Figure 5. Typical two-Maxwellian polar rain distribution function at low altitude (840 km).

Makita and Meng, 1987). Figure 6 was prepared using solar wind data (King, 1979) and DMSP particle data. It shows the variation in the solar wind velocity, ion density, ion temperature, and field magnitude (top four panels) and a daily value for the north and south polar rain energy flux and number flux (bottom two panels) for three full sectors (marked T and A and separated by vertical dashed lines) following the vernal equinox in 1979. The polar rain fluxes are taken within 5° of either magnetic pole. The preferred hemisphere clearly alternates from one pole to the other with sector change. This asymmetry is one of the strongest arguments for the direct entry model.

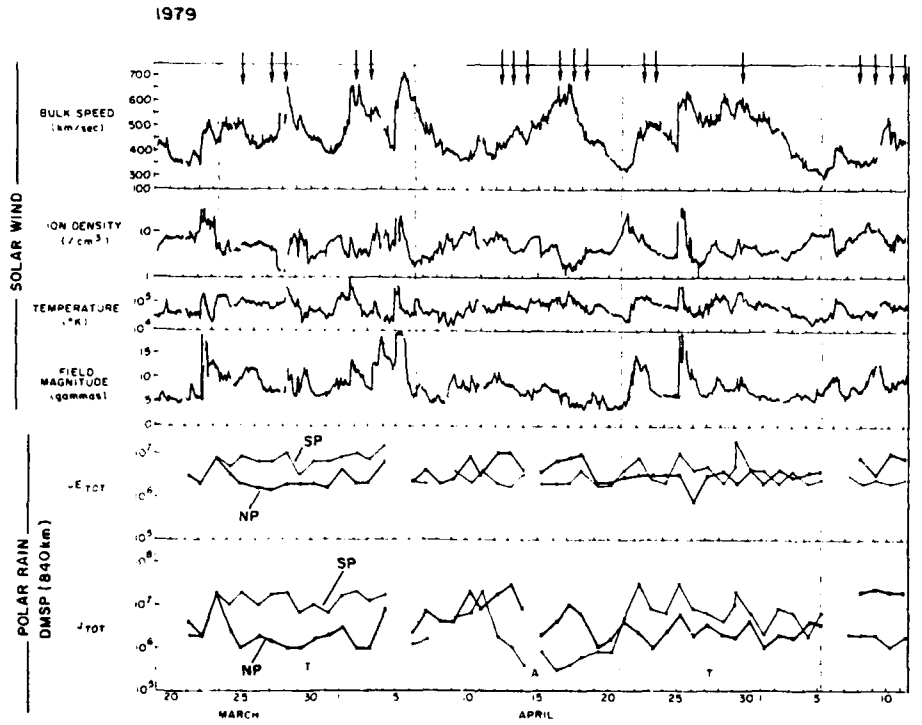

Figure 6. Variation of solar wind parameters and low altitude polar rain energy flux, JE_{TOT} in keV/(cm^2 s sr), and number flux, J_{TOT} in (cm$_2$ s sr)$^{-1}$, from 20 March to 11 May, 1979.

The two-dimensional morphology of polar rain in the preferred and non-preferred cap was statistically determined using DMSP electron data at 840 km by Gussenhoven et al. (1984). Maps were constructed in magnetic latitude and local time of the average polar rain characteristics using one year of data and separating the data by KP and by IMF sector. This study confirmed that the hemispheric, sector-dependent asymmetry in flux levels is also found in the average sense. When taken across the entire polar cap the total number flux input to the preferred hemisphere was approximately 2 times that in the non-preferred hemisphere.

Gussenhoven et al. also found that within a given cap there is a

large statistical variation from high to low flux along a prenoon to premidnight axis of symmetry. This variation (also evident in the top electron panel of Figure 4) is, on average, larger than the hemispheric asymmetry. Table 1 illustrates both the average day-night variation within a given cap and the hemispheric asymmetry. To construct Table 1 a Maxwellian fit was made to the average spectra shown in Gussenhoven et al. (1984) at two positions along the noon-midnight axis for the preferred and unpreferred caps. The left-hand comparison is for the dayside at 79° MLAT directly behind the cusp. The right-hand comparison is on the nightside at 75° MLAT above the midnight oval. On the dayside the average difference in density between hemispheres is a factor of 3, on the nightside it is a factor of 7. Furthermore, the day-night difference in density in the preferred cap is much less (a factor of 2.4) than that in the unpreferred cap (a factor of 6).

TABLE 1. Density (n) and temperature (kT) of polar rain along the noon-midnight axis, KP = 3-5+

	79° (noon)		75° (midnight)	
	$n(cm^{-3})$	kT(eV)	$n(cm^{-3})$	kT(eV)
Preferred	.22	79	.086	90
Unpreferred	.07?	55	.012	81

Gussenhoven et al. (1984) also identified a pronounced seasonal variation in polar rain flux. Not only is the peak flux higher in the summer than winter, but the region of high number flux extends much further across the caps in summer.

The direct entry mechanism does not easily provide a mechanism for cross-cap variation and seasonal dependence of polar rain flux. On the other hand, the internal barrier model is expected to produce a field-aligned potential drop having strong latitude and altitude dependencies.

Although a clear modulation of polar rain intensity has been shown to occur in a given hemisphere and between hemispheres with IMF sector, there has been little success in relating polar rain characteristics to other solar wind parameters (Riehl and Hardy, 1986; Makita and Meng, (1987). Figure 6 also demonstrates that no obvious relationship exists between the polar rain flux and solar wind parameters. Pilipp et al. (1987b) have shown that narrowly peaked strahl occurs in high speed solar wind streams which tend to occur in the middle of well-formed sectors. Such streams are often characterized by low solar wind density (see also Fairfield and Scudder, 1985). When the strahl is narrowly peaked the hemispheric asymmetry in polar rain flux should be greatest. Arrows at the top of Figure 6 mark instances where the hemispheric difference in polar rain number flux is an order of

magnitude or greater. These occur frequently, but not exclusively in high speed streams and periods of low density. This lack of a one-to-one correlation supports entry and transport mechanisms for polar rain in which some modification of the solar wind plasma occurs.

3. POLAR RAIN AND THE MANTLE POPULATION FROM 5-60 RE.

The electron populations in the lobes, which magnetically map to the polar caps, are far less systematically studied than the polar cap populations at low altitudes. Two particle populations are found at mid-altitudes in the lobe. One is the boundary population, including the plasma mantle. It is characterized by tailward streaming ions of moderately high density ($\sim$.5 cm^{-3}). The other is the plasma that is measured when the boundary plasma is not present. In this plasma ions above $\sim$50 eV are not detected. Weak electron fluxes >50 eV are measured, and it is these fluxes that are associated with low altitude polar rain.

One of the most interesting features of the 'polar rain' measurements beyond 5 RE is that while plasma mantle populations are explicitly excluded from study, no distinction is made between polar rain, polar shower and polar cap arc electron populations. In other words, no requirement on spatial/temporal smoothness or on IMF Bz conditions are imposed to identify polar rain at mid- to high altitudes.

Shortly after the identification of polar rain in low altitude data Yeager and Frank (1976) studied the >250 eV electron population in the northern lobes from 3-7 RE using Imp 5 data. Their 'polar cap' population was distinguished from interplanetary, magnetosheath, polar cusp, and plasma mantle electron populations. Their polar cap electron spectra are similar to the low altitude polar rain spectra and range in density from .0015-.045 cm^{-3}. They are isotropic within factors of 3 to 4. The variation of electron fluxes averaged over each northern polar cap crossing for ten months in 1970 showed systematic increases in away sectors. The enhancement between low and high fluxes in the energy range 305-510 eV varied between 2 and 50. There was no strong local time dependence in the fluxes. Ions between 80 eV and 50 keV were below detectability, putting an upper limit on density of .05 cm^{-3} in this energy range.

More recently Fairfield and Scudder (1985), using ISEE 1 data, examined the electron population in the northern tail lobe between 10-23 RE. They excluded from their study magnetopause boundary layer and plasma mantle populations. At times they found extended periods for which the fluxes of electrons above $\sim$100 eV were significantly greater both parallel and antiparallel to the magnetic field than perpendicular to the field indicating bidirectional streaming. An example of their data is shown in Figure 7 (taken from Greenspan et al., 1986). The ISEE 1 detector response during an intense polar rain event is given for various energy channels as a function of pitch angle. Dashed lines indicate background levels. In 399 hours of such data the anisotropy, defined as the ratio of the parallel to the perpendicular flux, was

found to be more pronounced during away sectors. In the 180 eV channel it was greater than 1.1 more than 90% of the time. For toward sectors it was greater than 1.1 only 13 % of the time. At this energy the ratio of the average flux in away sectors to that in toward sectors was 2.4. The authors concluded that the electron characteristics in the preferred hemisphere, namely, the bidirectional anisotropy and the enhanced flux, were clear signatures of the direct entry of an anisotropic strahl population in the solar wind and its adiabatic transport to low altitudes.

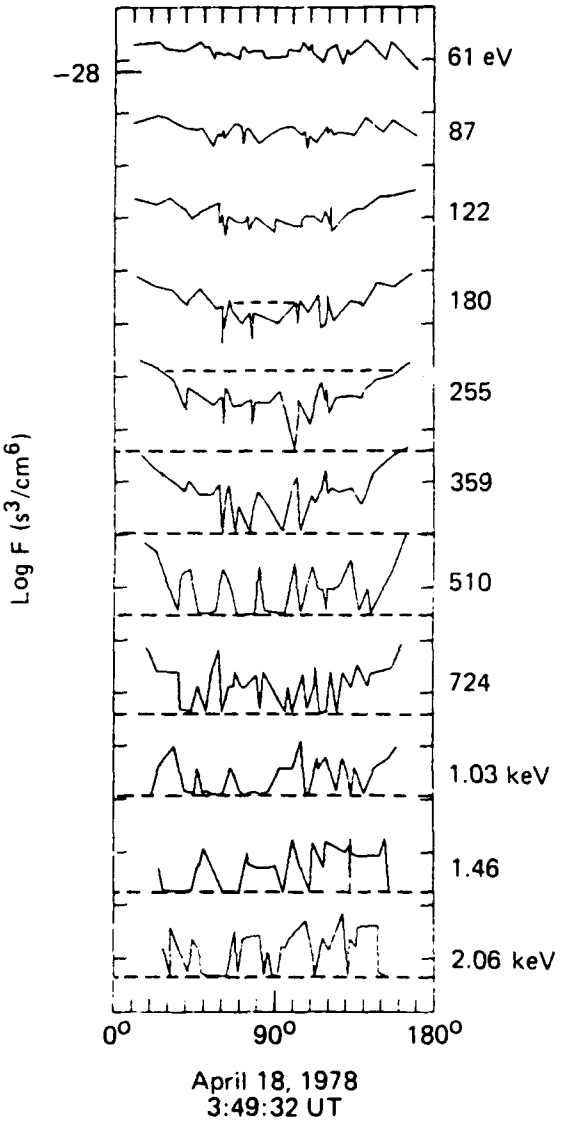

Figure 7. Polar rain pitch angle variations at ISEE 1 altitudes.

It should be noted that most of the cases reported by Fairfield and Scudder correspond to unusually intense polar rain events. These events are more readily compared to the events discussed by Foster and Burrows (1976, 1977) than to normally occurring polar rain. At low altitudes the keV electrons in intense events were also found to have a strong field alignment. Foster and Burrows (1977) successfully postulated a fluctuating magnetotail barrier potential to explain the measured pitch angle anisotropy. Recall that in the Foster and Burrows event there was no evidence of enhanced keV electron fluxes in simultaneous solar wind measurements.

In order to examine whether or not a potential drop exists from ISEE 1 altitudes to low altitudes, Greenspan et al. (1986) compared northern hemisphere electron spectra in intense polar rain events at ISEE 1 to those at DMSP. An example which typifies the DMSP-ISEE 1 comparisons, taken from Greenspan et al. is shown in Figure 8 for May 30, 1978. The angles marked are the pitch angles at which the ISEE 1 data were taken. For the most part the two spectra show very good agreement. There is no constant offset of one spectrum with respect to the other indicative of a potential drop between the two measurements. The tendency for high energy values of the distribution function at DMSP

(low altitude) to be higher than those at ISEE 1 (mid-altitude) was found in almost all cases. The suggested explanation for this is that the ISEE 1 detector does not adequately sample the strongly peaked loss cone population which maps adiabatically to DMSP altitudes.

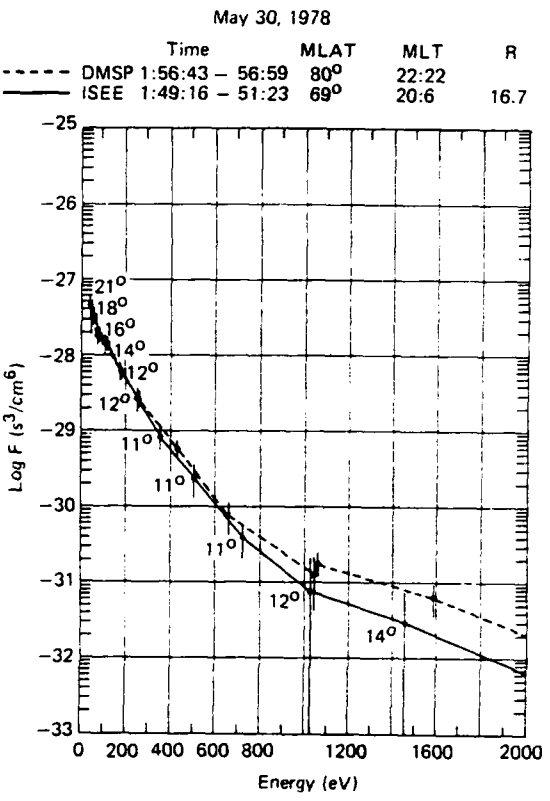

Figure 8. Comparison of low and mid-altitude polar rain spectra.

Before turning to high altitude tail lobe measurements some comments should be made concerning the electrons accompanying the tailward streaming ions in the mid-altitude boundary population. In the near-cusp mantle the electrons have magnetosheath characteristics, and are somewhat cooler and several orders of magnitude denser than the polar rain measurements of Yeager and Frank. The plasma mantle electrons do not show the strong velocity filter effects of ions and maintain reasonably constant characteristics well inward from the magnetopause where the ions cool systematically and fall below the energy range of the detector (Sckopke and Paschmann, 1978). At the moon the electrons accompanying the mantle ions are also hotter and denser than those of the polar rain population (Hardy et al., 1979b). Thus there is a clear bimodal distribution of tail lobe electrons in the altitude range of 0 to 60 RE. The bimodality is also evident in the statistical study of Zwickl et al. (1984) using ISEE 3 data from transfer orbit periods. Between 0-60 RE the electron density has two strong, near-equal peaks in occurrence frequency at .01 cm^{-3} and .4 cm^{-3}. The temperature is singly peaked at ∿80 eV but has a broad tail at lower values. On average the electrons are found to be weakly streaming away from the Earth.

Of major importance here is that the two tail lobe plasma populations share magnetic field lines. The denser boundary plasma fans out down-tail, occupying field lines that when mapped back to lower altitudes contain only the near-background polar rain electrons. Thus the populations at 60 RE on a given field line are not those adiabatically mapped to 1-10 RE on the same field line. They are constrained from reaching those altitudes by convection and down-tail streaming. The distance at which the electron pressure on a field line begins to substantially deviate from polar rain values is apparently greater than

10-23 RE since out to these distances the Greenspan et al. (1986) comparisons showed good agreement.

4. TAIL LOBE ELECTRONS AT HIGH ALTITUDES

The positioning of ISEE 3 in the distant tail made possible the collection of a large body of data on the plasmas and fields found there. One of the principal findings from these data is that the tail lobes and the plasma sheet are well-defined to distances exceeding 200 RE.

In comparing tail lobe electron characteristics at high altitudes and low altitudes, both statistically and on a case by case basis, it was found that the high altitude populations are much denser. The statistical study of Zwickl et al. (1984) showed that for >180 RE the frequency of occurrence of densities between .05 and 3 cm^{-3} is almost constant, and the peak at low densities (.01 cm^{-3}), associated with polar rain, is missing. The temperature profiles from low to high altitudes cool slightly from peak occurrence at 80 eV to peak occurrence at 54 eV. Baker et al. (1987) compared tail lobe electron spectra from ISEE 3 near 200 RE to DMSP polar rain spectra. A sample comparison for northern and southern hemispheres on 24 January, 1983 is

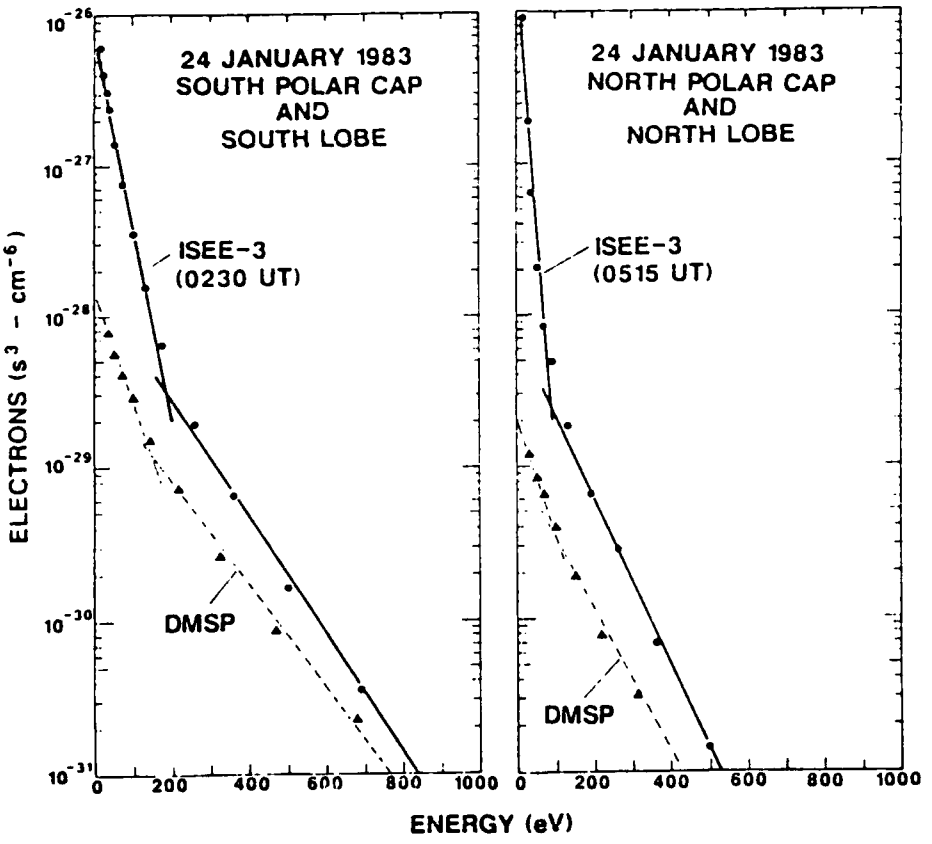

Figure 9. Comparison of low and high altitude polar rain spectra.

shown in Figure 9. The ISEE 3 distributions were measured as close as possible to field-alignment under relatively steady conditions. The DMSP data were taken near the magnetic pole and were long term averages. Because of a clear break-point in the ISEE 3 data the distributions were fit to two Maxwellians above and below 200 eV. The low energy portion of the DMSP data is quite different than that at ISEE 3, being both far less intense (by orders of magnitude) and warmer. The temperature of the high energy component is nearer that measured at ISEE 3 but again the intensity is much lower. Because the displacement of the ISEE 3 high energy distribution function value is fairly uniform by an amount 100-150 eV the comparison of the two spectra is suggestive of a potential drop between the two by that amount.

Figure 9 also shows that the electron population in the tail lobes has a greater intensity in the preferred hemisphere as does the polar rain at low altitudes. Gosling et al. (1985) studied 21 rapid crossings from the tail lobe in one hemisphere to the tail lobe in the other hemisphere and found that the morning sector density was 3-10 times higher in the northern (southern) hemisphere for IMF away (toward) sectors. The preferred hemisphere was in the opposite sense in the one evening side passage for which there were IMF data.

Baker et al. (1984) found not only that the preferred hemisphere for tail lobe fluxes was the same as for low altitude polar rain, but that the higher fluxes exhibited strong bidirectional streaming or field-aligned pitch angle anisotropies similar to that found in the mid-altitude polar rain data of Fairfield and Scudder (1985). Furthermore, examining cases where ISEE 3 passed rapidly from the tail lobe to the magnetosheath, they found that the spectrum for electrons streaming away from the sun in the magnetosheath was nearly identical to that for electrons streaming toward the Earth in the tail lobe. Figure 10 shows their example of this. On the left are two examples of electron pitch angle distributions for a variety of energy channels. The top, left panel is taken in the magnetosheath, and the first set of peaked count rates is in the field-aligned direction and away from the sun. The bottom left panel is in the tail lobe some ten minutes later, and the first set of peaked count rates is field-aligned and toward the Earth. The most field-aligned spectra are compared on the right. The two spectra are consistently separated from each other by at most 10 eV, which the authors consider the extent of the potential barrier in crossing from the magnetosphere to the magnetosheath. They feel that this comparison rather convincingly proves direct entry. One notes, however, that the tail lobe plasma flowing from the Earth (reflected plasma in the direct entry picture) is more intense than that flowing from the source toward the Earth, and that while the antisunward streaming magnetosheath plasma may be interpreted as having easy entry into the magnetosphere, the reflected, tailward streaming magnetosheath plasma does not get out.

To conclude this section we compare electron spectra taken in the magnetosheath and solar wind to those at low altitude in the polar cusp and polar cap on 9 October, 1984. The comparison is shown in Figure 11. The data outside the magnetopause were taken aboard the AMPTE/UKS

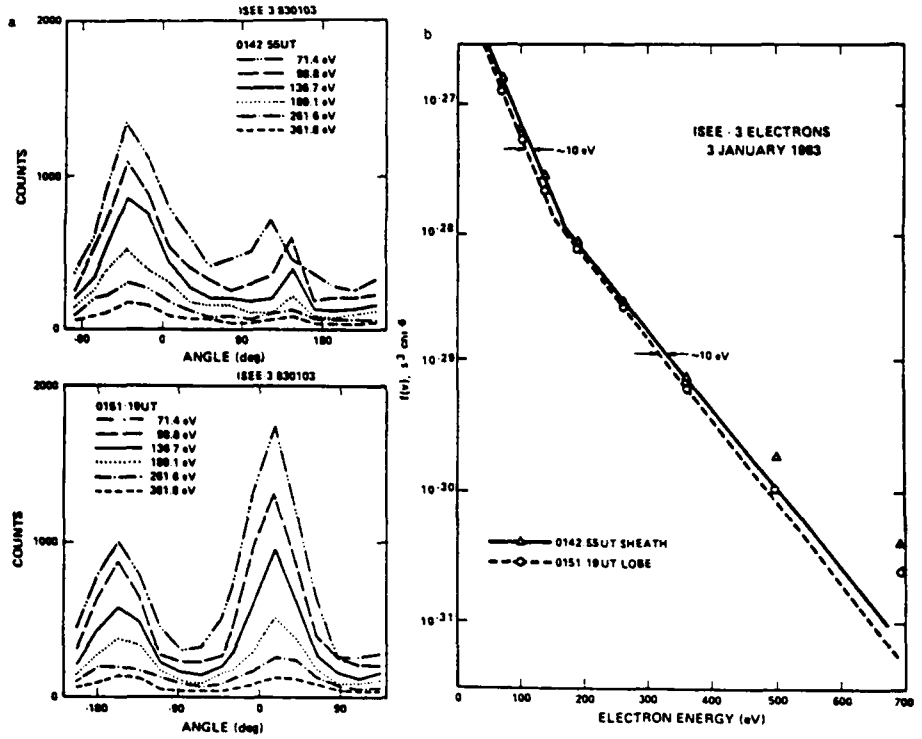

Figure 10. Magnetosheath and tail lobe pitch angle variations (left) and comparison of the two spectra at the most field aligned position.

satellite (David Hall, private communication, 1988) at low inclination on the dayside. The spectra were constructed from 20 minute averages of data. For the solar wind, average spectra parallel, antiparallel and perpendicular to the IMF are shown. A single magnetosheath spectrum is given because it is nearly isotropic. The low altitude precipitating electron data were taken aboard the DMSP satellites. The cusp spectrum is taken near local noon during the time of the AMPTE/UKS magnetosheath measurement and is averaged for 1 minute. The polar rain spectra are constructed from daily averages of data taken near the magnetic pole in either hemisphere.

The following spectral comparisons can be made: Above 50 eV the magnetosheath spectrum bears little resemblance to the solar wind spectra. It is more intense and falls off much faster from its peak value. Below 50 eV, however, the comparison is good. The cusp and magnetosheath spectra have the most favorable comparison, both being quasi-thermal with temperatures near 100 eV. The cusp spectrum is lower in intensity than the sheath spectrum below 500 eV and higher above. The solar wind and the polar rain spectra compare favorably in shape above 300 eV, but the polar rain intensity is at least an order of magnitude less in intensity. In the 100 eV range the polar rain

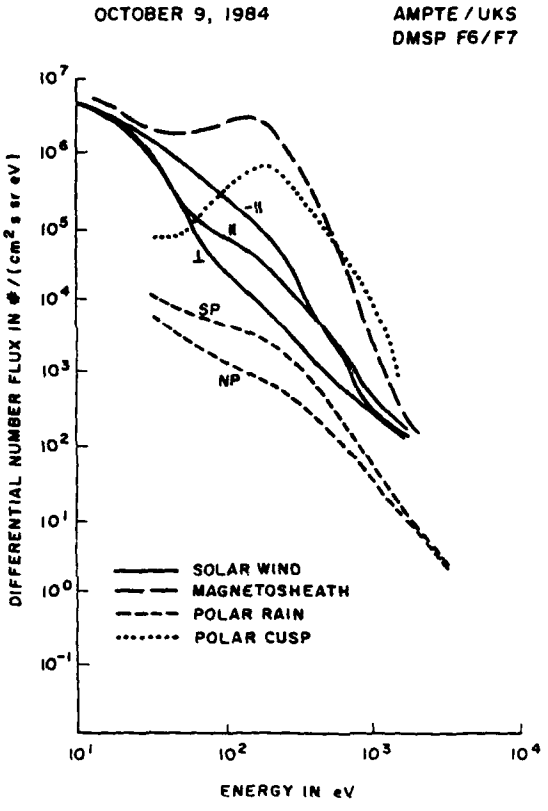

Figure 11. Comparison of solar wind, magnetosheath, polar cusp and polar rain spectra on 9 October, 1984.

spectra are considerably warmer than the solar wind spectra. In sum, the processes required to produce any one of these spectra from any other one must be complex. No straight-forward process, such as direct entry or field-aligned acceleration can account for the spectral differences.

5. CONCLUSIONS

Within the magnetosphere the weakest plasma occurs in the most simply configured magnetic field region, namely the tail lobes. The apparent simplicity of the tail lobes tempts us to ignore internal lobe processes and use the lobes as pass-through regions for information about more complicated processes such as the solar wind-magnetosphere interactions or those in the solar corona. The direct entry model of the solar wind plasma allows us to do this, and is highly attractive because of it. Recent measurements in the near to far tail lobes indicate that such a simple picture is premature.

Statistical studies show that the tail lobes become increasingly more dense with increasing distance downtail. The extremely weak

electron populations are apparently only common at low and mid-altitudes. Even at mid-altitudes the boundary plasma in regions of strong convection fills much of the lobes. In the distant tail it is rare to find regions where the electron density is extremely weak. Plasma measurements there indicate that the magnetopause is leaky and rather efficiently lets in magnetosheath plasma. Thus a single polar cap field line could conceivably pass through a low altitude region of weak polar rain electrons, a comparatively dense, somewhat warmer plasma mantle population, another rarified region beyond the plasma mantle, and then into an increasingly denser magnetosheath type population before exiting the magnetosphere. The pressure changes along the field line in this scenario would most certainly be accompanied by field-aligned potential differences.

The preferred hemisphere dependence on IMF for low and mid-altitude polar rain intensity and for pitch angle anisotropy is convincing evidence for direct entry of the solar wind strahl. A remaining concern is whether or not the hemispheric difference in the polar rain fits the characteristics of the backstreaming solar wind electron population. On average the difference in intensity between polar rain in the preferred and non-preferred hemispheres is considerably less than that found in the anisotropic strahl measurements. It also remains to be shown that hemispheric polar rain differences match solar wind strahl anisotropies on a case by case comparison. Occurrence conditions for highly anisotropic strahl have not been shown to be the same as those for either intense polar rain events, or for polar rain events with large hemispheric differences.

Tail lobe plasma electrons beyond some undetermined altitude apparently cease to change character as a function of IMF Bz. At lower altitudes one can nearly predict the sign of Bz by the change from polar rain to polar showers or polar cap arcs. Furthermore, strong local time and seasonal dependencies seem to be much more pronounced at low altitudes than at high altitudes. One should be cautious here because of the difficulty in obtaining sufficient data to make these comparisons in the distant tail. Nevertheless, these dependencies are far more suggestive of a gating mechanism operating in the lobes that allows more or less plasma through from high altitudes to low altitudes. Such a mechanism could be one or more field-aligned potential drops, each driven separately. Thus there are indications of the existence of field-aligned potential differences at high latitudes, but as yet no clear method for producing them has gained acceptance.

On the one hand, we have a simple and elegant model for polar rain, direct entry, which cannot explain many of the polar rain characteristics in detail. On the other, we have the internal barrier model which requires quantification in order to gain any foothold. In reality a combination of both models may be required to fully explain tail lobe dynamics. Progress can be made by considering the following questions: What are the characteristics of the ion lobe population as a function of altitude? Are the ion and electron populations as we understand them hydromagnetically self-consistent? How important is the convection electric field in the distant tail and what is the

source of the IMF sector dependence of the lobe plasma density there? If there are field-aligned potential differences, how do they couple to the ionosphere? And if there is direct entry of the strahl, why does it, unlike the rest of the solar wind plasma, escape perturbation by the bow shock? It is incumbent upon us, therefore, to be dissatisfied with excessively simple pictures that lead us away from the opportunity to understand a complex situation, even if the complex situation is one of the easier ones presented to us in magnetospheric physics.

ACKNOWLEDGEMENTS

I wish to express my appreciation to David S. Hall of the Rutherford Appleton Laboratory for providing the AMPTE/UKS data and to Gary Mullen and David Hardy at the Air Force Geophysics Laboratory for continuing discussions on polar cap dynamics and insightful comments on the manuscript.

REFERENCES

Baker, D.N., S.J. Bame, W.C. Feldman, J.T. Gosling, R.D. Zwickl, J.A. Slavin, and E.J. Smith, J. Geophys. Res., 91, 5637, 1986.

Baker, D.N., S.J. Bame, J.T. Gosling, and M.S. Gussenhoven, J. Geophys. Res., 92, 13,547, 1987.

Fairfield, D.H., and J.D. Scudder, J. Geophys. Res., 90, 4055, 1985.

Feldman, W.C., J.R. Asbridge, S.J. Bame, M.D. Montgomery and S.P. Gary, J. Geophys. Res., 80, 4181, 1975.

Fennell, J.F., P.F. Mizera, and D.R. Croley, Proc. Int. Conf. Cosmic Rays 14th, 4, 1267, 1975.

Foster, J. C., and J. R. Burrows, J. Geophys. Res., 81, 6016, 1976.

Foster, J. C., and J. R. Burrows, J. Geophys. Res., 82, 5165, 1977.

Gosling, J.T., D.N. Baker, S.J. Bame, W.C. Feldman, and R.D. Zwickl, J. Geophys. Res., 90, 6354, 1985.

Gosling, J.T., D.N. Baker S.J. Bame, and R.D. Zwickl, J. Geophys. Res., 91, 11352, 1986.

Greenspan, M.E., C.-I. Meng and D.H. Fairfield, J. Geophys. Res., 91, 11,123, 1986.

Gussenhoven, M.S., J. Geophys. Res., 87, 2401, 1982.

Gussenhoven, M.S., D.A. Hardy, N. Heinemann, and R.K. Burkhardt, J. Geophys. Res., 89, 9785, 1984.

Hardy, D.A., J. Geophys. Res., 89, 3883, 1984.

Hardy, D.A., H.K. Hills, and J.W. Freeman, J. Geophys. Res., 84, 72, 1979a.

Hardy, D.A., P.H. Reiff, and W.J. Burke, J. Geophys. Res., 84, 1382, 1979b.

King, J.H., Rep. NSSDC 79-08, NASA Goddard Space Flight Center, Greenbelt, MD., 1979.

Makita, K. and C.-I Meng, J. Geophys. Res., 92, 7381, 1987.

Meng, C.-I. and H.W. Kroehl, J. Geophys. Res., 82, 2305, 1977.

Olbert, S., Eur. Space Agency Spec. Publ., SP-161, 135, 1981.
Paulikas, G.A., Rev. Geophys. Space Phys., 12, 117, 1974.
Pilipp, W.G., H. Miggenrieder, M.D. Montgomery, K.-H. Muhlhauser, H. Rosenbauer and R. Schwenn, J. Geophys. Res., 92, 1075, 1987a.
Pilipp, W.G., H. Miggenrieder, K.-H. Muhlhauser, H. Rosenbauer and R. Schwenn, and F.M. Neubauer, J. Geophys. Res., 92, 1103, 1987b.
Pilipp, W.G., and G. Morfill, J. Geophys. Res., 83, 5670, 1978
Riehl, Kevin B. and David A. Hardy, J. Geophys. Res., 91, 1557, 1986.
Rosenbauer, H., H. Grunwaldt, M.D. Montgomery, G. Paschmann, and N. Sckopke, J. Geophys. Res., 80, 2723, 1975.
Sckopke, N., and G. Paschmann, J. Atmos. Terr. Phys., 40, 261, 1978.
Yeager, D.M. and L.A. Frank, J. Geophys. Res., 81, 3966, 1976.
Winningham, J.D. and W.J. Heikkila, J. Geophys. Res., 79 949, 1974.
Zwickl, R.D., D.N. Baker, S.J. Bame, W.C. Feldman, J.T. Gosling, E.W. Hones, Jr., D.J. McComas, B.T. Tsurutani, and J.A. Slavin, J. Geophys. Res., 89, 11007, 1984.